Research Article
Experimental and Translational Hepatology

JOURNAL
OF HEPATOLOGY

Downregulation of TGR5 (GPBAR1) in biliary epithelial cells contributes to the pathogenesis of sclerosing cholangitis

Graphical abstract

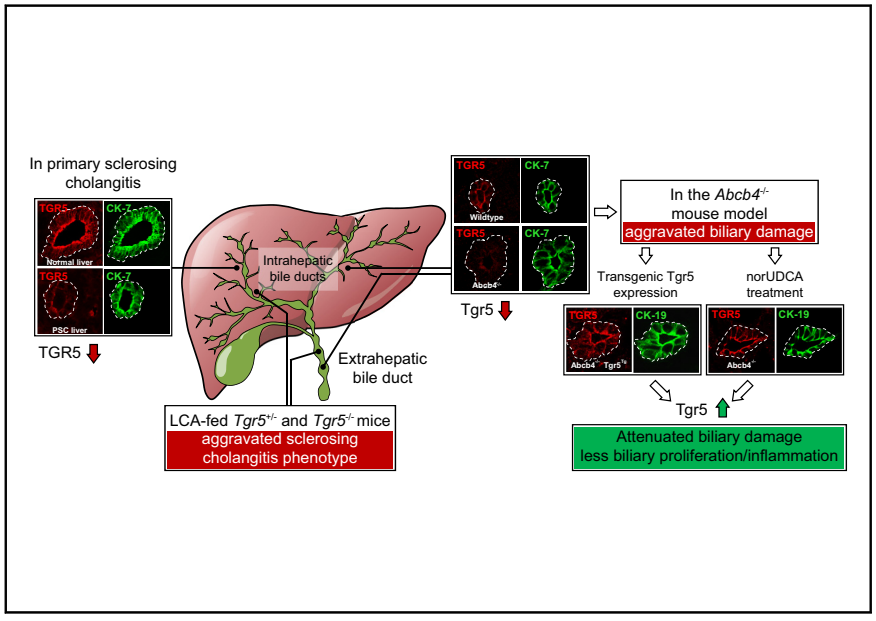

Highlights

- TGR5 is downregulated in cholangiocytes in PSC and *Abcb4*$^{-/-}$ livers in a cell type-specific manner.
- Interleukin-8 reduces TGR5 levels in biliary epithelial cells and biliary organoids.
- Biliary damage is aggravated in Tgr5-deficient mice and is attenuated in *Abcb4*$^{-/-}$ mice overexpressing Tgr5.
- ScRNA-seq shows that overexpression of Tgr5 in *Abcb4*$^{-/-}$ mice ameliorates the activated, inflammatory biliary phenotype.
- norUDCA treatment restores biliary Tgr5-expression in *Abcb4*$^{-/-}$ mice.

Authors

Maria Reich, Lina Spomer, Caroline Klindt, …, Tom Luedde, Mathias Heikenwalder, Verena Keitel

Correspondence

verena.keitel@med.uni-duesseldorf.de (V. Keitel).

Lay summary

Primary sclerosing cholangitis (PSC) is a chronic cholestatic liver disease-associated with progressive inflammation of the bile duct, leading to fibrosis and end-stage liver disease. Bile acid (BA) toxicity may contribute to the development and disease progression of PSC. TGR5 is a membrane-bound receptor for BAs, which is found on bile ducts and protects bile ducts from BA toxicity. In this study, we show that TGR5 levels were reduced in bile ducts from PSC livers and in bile ducts from a genetic mouse model of PSC. Our investigations indicate that lower levels of TGR5 in bile ducts may contribute to PSC development and progression. Furthermore, treatment with norUDCA, a drug currently being tested in a phase III trial for PSC, restored TGR5 levels in biliary epithelial cells.

https://doi.org/10.1016/j.jhep.2021.03.029
 J. Hepatol. 2021, 75, 634–646

Research Article
Experimental and Translational Hepatology

JOURNAL OF HEPATOLOGY

Downregulation of TGR5 (GPBAR1) in biliary epithelial cells contributes to the pathogenesis of sclerosing cholangitis

Maria Reich[1,†], Lina Spomer[1,†], Caroline Klindt[1], Katharina Fuchs[1], Jan Stindt[1], Kathleen Deutschmann[1], Johanna Höhne[1], Evaggelia Liaskou[2,3], Johannes R. Hov[4,5], Tom H. Karlsen[4,5], Ulrich Beuers[6], Joanne Verheij[6], Sofia Ferreira-Gonzalez[7], Gideon Hirschfield[8], Stuart J. Forbes[7], Christoph Schramm[9], Irene Esposito[10], Dirk Nierhoff[11], Peter Fickert[12], Claudia Daniela Fuchs[13], Michael Trauner[13], María García-Beccaria[14], Gisela Gabernet[15], Sven Nahnsen[15], Jan-Philipp Mallm[16], Marina Vogel[17], Kristina Schoonjans[18], Tobias Lautwein[19], Karl Köhrer[19], Dieter Häussinger[1], Tom Luedde[1], Mathias Heikenwalder[14], Verena Keitel[1,*]

[1]*Department of Gastroenterology, Hepatology and Infectious Diseases, University Hospital Düsseldorf, Medical Faculty of Heinrich Heine University Düsseldorf, Moorenstr. 5, 40225 Düsseldorf, Germany;* [2]*Centre for Liver and Gastrointestinal Research, Institute of Immunology and Immunotherapy, University of Birmingham, Birmingham, UK;* [3]*NIHR Birmingham Biomedical Research Centre, University Hospitals Birmingham NHS Foundation Trust, Birmingham, UK;* [4]*Norwegian PSC Research Centre and Section of Gastroenterology at the Department of Transplantation Medicine, and Research Institute of Internal Medicine, Division of Cancer Medicine, Surgery and Transplantation, Oslo University Hospital, Rikshospitalet, Oslo, Norway;* [5]*Institute of Clinical Medicine, Faculty of Medicine, University of Oslo, Oslo, Norway;* [6]*Department of Gastroenterology and Hepatology and Tytgat Institute for Liver and Intestinal Research and Department of Pathology, Amsterdam University Medical Centers, Location AMC, AGEM Amsterdam, The Netherlands;* [7]*Centre for Regenerative Medicine, University of Edinburgh, UK;* [8]*Toronto Centre for Liver Disease, Toronto General Hospital, Toronto, Canada;* [9]*I. Department of Medicine and Martin Zeitz Centre for Rare Diseases, University Medical Center Hamburg-Eppendorf, Hamburg, Germany;* [10]*Institute of Pathology, University Hospital Düsseldorf, Medical Faculty of Heinrich Heine University Düsseldorf, Moorenstr. 5, 40225 Düsseldorf, Germany;* [11]*Department of Gastroenterology and Hepatology, University of Cologne, Cologne, Germany;* [12]*Division of Gastroenterology and Hepatology, Department of Internal Medicine, Medical University of Graz, Graz, Austria;* [13]*Hans Popper Laboratory of Molecular Hepatology, Division of Gastroenterology and Hepatology, Department of Internal Medicine III, Medical University of Vienna, Vienna, Austria;* [14]*Division of Chronic Inflammation and Cancer, German Cancer Research Center Heidelberg (DKFZ), Heidelberg, Germany;* [15]*Quantitative Biology Center (QBiC), Eberhard-Karls University of Tübingen, Tübingen, Germany;* [16]*Single Cell Open Lab, German Cancer Research Center Heidelberg (DKFZ), Heidelberg, Germany;* [17]*DKFZ Genomics and Proteomics Core Facility, German Cancer Research Center Heidelberg (DKFZ), Heidelberg, Germany;* [18]*Laboratory of Metabolic Signaling, Institute of Bioengineering, School of Life Sciences and School of Engineering, École Polytechnique Fédérale de Lausanne, Lausanne, Switzerland;* [19]*Genomics and Transcriptomics Laboratory, Biologisch-Medizinisches-Forschungszentrum (BMFZ), Heinrich Heine University Düsseldorf, Germany*

Background & Aims: Primary sclerosing cholangitis (PSC) is characterized by chronic inflammation and progressive fibrosis of the biliary tree. The bile acid receptor TGR5 (GPBAR1) is found on biliary epithelial cells (BECs), where it promotes secretion, proliferation and tight junction integrity. Thus, we speculated that changes in TGR5-expression in BECs may contribute to PSC pathogenesis.

Methods: TGR5-expression and -localization were analyzed in PSC livers and liver tissue, isolated bile ducts and BECs from *Abcb4*$^{-/-}$, *Abcb4*$^{-/-}$/*Tgr5*^{Tg} and ursodeoxycholic acid (UDCA)- or 24-norursodeoxycholic acid (norUDCA)-fed *Abcb4*$^{-/-}$ mice. The effects of IL8/IL8 homologues on TGR5 mRNA and protein levels were studied. BEC gene expression was analyzed by single-cell transcriptomics (scRNA-seq) from distinct mouse models.

Results: TGR5 mRNA expression and immunofluorescence staining intensity were reduced in BECs of PSC and *Abcb4*$^{-/-}$ livers, in *Abcb4*$^{-/-}$ extrahepatic bile ducts, but not in intrahepatic macrophages. No changes in TGR5 BEC fluorescence intensity were detected in liver tissue of other liver diseases, including primary biliary cholangitis. Incubation of BECs with IL8/IL8 homologues, but not with other cytokines, reduced TGR5 mRNA and protein levels. BECs from *Abcb4*$^{-/-}$ mice had lower levels of phosphorylated Erk and higher expression levels of Icam1, Vcam1 and Tgfβ2. Overexpression of Tgr5 abolished the activated inflammatory phenotype characteristic of *Abcb4*$^{-/-}$ BECs. NorUDCA-feeding restored TGR5-expression levels in BECs in *Abcb4*$^{-/-}$ livers.

Conclusions: Reduced TGR5 levels in BECs from patients with PSC and *Abcb4*$^{-/-}$ mice promote development of a reactive BEC phenotype, aggravate biliary injury and thus contribute to the pathogenesis of sclerosing cholangitis. Restoration of biliary TGR5-expression levels represents a previously unknown mechanism of action of norUDCA.

Keywords: bile acid receptor; interleukin-8; biliary damage; biliary organoids; scRNA-seq; norUDCA.
Received 25 May 2020; received in revised form 24 March 2021; accepted 25 March 2021; available online 17 April 2021
* Corresponding author. Address: Clinic for Gastroenterology, Hepatology and Infectious Diseases, University Hospital Duesseldorf, Medical Faculty of the Heinrich Heine University Duesseldorf, Moorenstrasse 5, D-40225 Duesseldorf, Germany; Fax: (49) 211 8118752; Tel.: (49) 211 8116330.
E-mail address: verena.keitel@med.uni-duesseldorf.de (V. Keitel).
† These authors contributed equally to this work
https://doi.org/10.1016/j.jhep.2021.03.029

Lay summary: Primary sclerosing cholangitis (PSC) is a chronic cholestatic liver disease-associated with progressive inflammation of the bile duct, leading to fibrosis and end-stage liver disease. Bile acid (BA) toxicity may contribute to the development and disease progression of PSC. TGR5 is a membrane-bound receptor for BAs, which is found on bile ducts and protects bile ducts from BA toxicity. In this study, we show that TGR5 levels were reduced in bile ducts from PSC livers and in bile ducts from a genetic mouse model of PSC. Our investigations indicate that lower levels of TGR5 in bile ducts may contribute to PSC development and progression. Furthermore, treatment with norUDCA, a drug currently being tested in a phase III trial for PSC, restored TGR5 levels in biliary epithelial cells.

Introduction

Primary sclerosing cholangitis (PSC) is a rare cholestatic liver disease characterized by chronic inflammation and progressive fibrosis of the intrahepatic and extrahepatic bile ducts.[1–3] There is an increased risk of hepatic malignancy, mainly cholangiocarcinoma.[1–3] Genetic, environmental and immunological risk factors, dysregulation of the intestinal microbiota and the gut-liver axis, changes in bile composition and in biliary epithelial cell (BEC) phenotype have all been implicated in PSC aetiology.[2–6] Currently, no drug therapy has been approved for PSC.

Mice lacking the phospholipid-floppase Mdr2 (*Abcb4*$^{-/-}$) recapitulate the progressive fibrosing cholangitis aspect of human PSC and also develop intrahepatic malignancy.[4,7] Thus, *Abcb4*$^{-/-}$ mice are widely used as a model for sclerosing cholangitis. Feeding of the hydrophobic bile acid (BA) lithocholic acid (LCA, 1%w/w) results in destructive cholangitis and periductal fibrosis within 2-4 days in wild-type (WT) mice.[8] While this model resembles the biliary changes observed in PSC, LCA administration cannot be tolerated long-term.[7,8]

Takeda G protein-coupled receptor-5 (TGR5, also known as GPBAR1) is a G protein-coupled receptor responsive to both primary and secondary BAs.[9–12] TGR5 is expressed throughout the biliary tree in rodents and humans and has been detected in BECs lining small and large intrahepatic ducts, extrahepatic ducts and gallbladder epithelium.[13–17] Activation of TGR5 in BECs stimulates cyclic AMP generation leading to increased chloride and bicarbonate secretion resulting in bicarbonate-rich choleresis.[14,18–21] Furthermore, TGR5 contributes to BEC tight junction integrity.[22] Thus, TGR5 protects BECs from BA toxicity, explaining the significantly diminished viability of Tgr5-deficient BECs after BA challenge.[17] TGR5 activation also promotes BEC proliferation, which was attenuated in *Tgr5*$^{-/-}$ mice in models of cholestasis.[17] The prominent expression of TGR5 in BECs and the receptor's involvement in biliary secretion, cytoprotection and proliferation underlined the physiological need for TGR5 in this compartment, and indicated that it could have a role in the pathogenesis of cholangiopathies. Further evidence for a potential role of TGR5 in PSC stems from genome-wide association studies: a gene locus associated with both ulcerative colitis and PSC encompasses the *TGR5* gene locus.[23,24] Whether changes in TGR5-expression, localization and function in BECs contribute to PSC pathogenesis has not been fully elucidated.

The aims of the present study were fourfold: i) to investigate alterations in TGR5-expression and localization in BECs from PSC and *Abcb4*$^{-/-}$ livers, ii) to identify potential regulators of TGR5 in BECs in the context of sclerosing cholangitis, iii) to explore whether the absence of TGR5 predisposes to sclerosing cholangitis, while overexpression of TGR5 attenuates sclerosing cholangitis and iv) to identify potential therapeutic strategies.

Materials and methods

Human liver tissue

The study was performed according to the guidelines of the declaration of Helsinki. Informed written consent was obtained from all patients. For details see the supplementary information.

Animals/animal procedures

Abcb4$^{+/-}$ mice (BALB/c) were bred to obtain littermate *Abcb4*$^{-/-}$ and Abcb4$^{+/+}$ controls. *Tgr5*-transgenic (*Tgr5*^{Tg}) and *Tgr5* WT mice (C57BL/6J) were described elsewhere.[25] Both sexes (6–8-week-old) were used for experiments. Breeding was carried out with heterozygous animals to obtain littermate controls. 8-week-old male *Abcb4*$^{-/-}$ mice (FVB/N) were from Jackson Laboratory (Bar Habor, ME). Animals received either control diet (SAFE-diets, France) or a diet supplemented with 0.5% (w/w) ursodeoxycholic acid (UDCA) or 24-norursodeoxycholic acid (norUDCA) for 4 weeks. The experimental protocols were approved by the local Animal Care and Use Committee (BMWFW-66.009/0008-WF/V/3b/2015). Animals received humane care, were maintained on 12 h light/dark-cycle and had access to water and food *ad libitum*.

Isolation of human biliary epithelial cells

Human BECs were isolated as described.[26] Cells were treated at passage 4 with recombinant human IL8 (5 ng/ml) for 24 h before harvesting for protein extraction (see supplementary information).

Generation of human biliary organoids

Human biliary organoids were generated from cells contained in bile (2-10 ml) collected during endoscopic retrograde cholangiography.[27] The study protocol was approved by the ethical committee of the University Hospital Duesseldorf. Informed written consent was obtained from all patients.

Isolation and culture of murine BECs

BECs were isolated from livers of 6-8 week-old male and female mice.[15,17] For details including FACS enrichment see supplementary information.[28,29]

Single-cell experiments, 10x sample processing, library preparation and sequencing

Single-cell experiments were performed in 2 sets: *Abcb4*$^{-/-}$ and WT littermates; (Balb/c background) *Abcb4*$^{-/-}$/*Tgr5*^{WT} and *Abcb4*$^{-/-}$/*Tgr5*^{Tg} littermates (BALB/c x C57BL/6J). After FACS sorting for epithelial cell adhesion molecule (EpCAM), a total of 10,000 cells were used as input for the single-cell droplet libraries generation on the 10X Chromium Controller system utilizing the Chromium Single-Cell 3'NextGEM Reagent-Kit-v3.1 (10X Genomics, Pleasanton, CA). Sequencing was carried out on a NextSeq-550 system (Illumina Inc. San Diego, CA) with a mean sequencing depth of ~50,000 reads/cell.

Single-cell RNA-seq data analysis

CellRanger analysis pipeline (v5.0.0) was used to process the 10x genomics single-cell RNA-sequencing data: read alignment to the reference and generate a matrix containing UMI counts per gene per cell (gene expression matrix). The gene expression matrix was further processed using R[30] and the Seurat R-package (v3.2.2).[31] For cell clustering, the k-nearest neighbors of each cell were determined. An SNN (shared nearest neighbor) graph was constructed computing the Jaccard Index (neighborhood overlap) between each cell and its 20 nearest neighbors in the principal component space. The cell clusters were visualized using the uniform manifold approximation and projection (UMAP) technique.[32] Differential gene expression between cell clusters was determined by the Wilcoxon rank sum test. The resulting *p* values were adjusted using a Bonferroni correction. The significance threshold was set to 0.05. Additionally, a threshold of 0.25 was applied to the average log fold change expression. For details see the supplementary information.

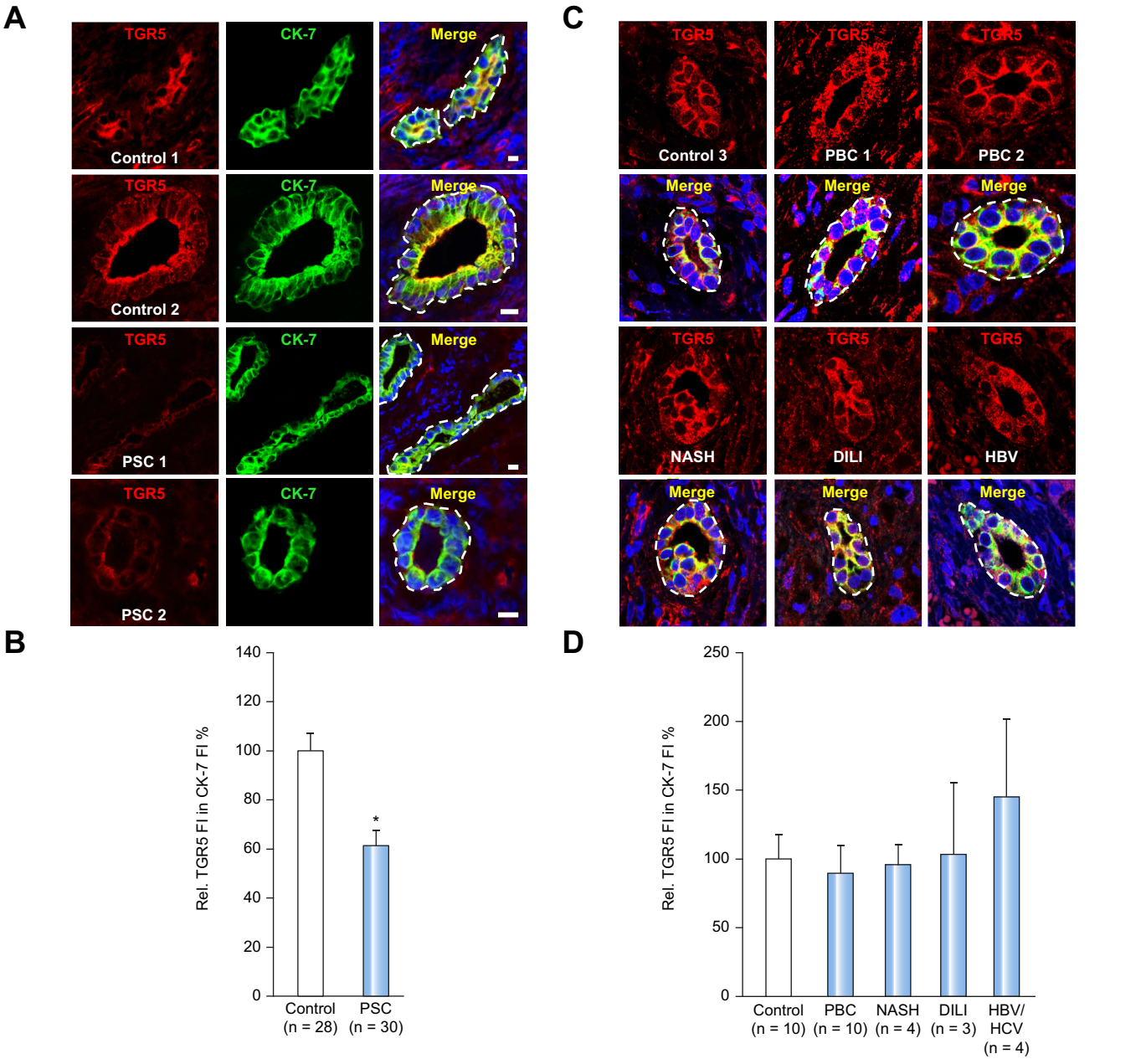

Fig. 1. TGR5 fluorescence intensity is reduced in BECs of PSC liver biopsies. (A) Liver tissue from controls and patients with PSC were double-labelled for TGR5 and CK-7. (B) TGR5 FI was determined in CK-7-positive BECs by densitometric analysis and expressed in relation to CK-7 FI (control livers n = 28 were set to 100%, PSC livers n = 30). (C) Liver tissue from patients with PBC (n = 10), NASH (n = 4), DILI (n = 3) and viral hepatitis (n = 4) was double-labelled for TGR5 and CK-7. (D) TGR5 FI was determined in CK-7-positive BECs by densitometric analysis and expressed in relation to CK-7 FI (controls set to 100%). Nuclei in A/C were stained with Hoechst. Bars = 10 μm. Data are shown as mean ± SEM; *significantly different to control livers (p <0.05, Mann-Whitney U test). BECs, biliary epithelial cells; DILI, drug-induced liver injury; FI, fluorescence intensity; NASH, non-alcoholic steatohepatitis; PBC, primary biliary cholangitis; PSC, primary sclerosing cholangitis.

Western blotting
Cells and liver tissue were lysed as described.[14,17]

Image acquisition and expression analysis
Confocal images were acquired on a Zeiss laser scanning microscope 510META or Model880 equipped with a 63xPlan Neofluar objective using ZEN-software (black edition-Ver.2.3-SP1). For image acquisition parameters/image analysis see supplementary information.

Statistical analysis
Results were analyzed using the non-parametric 2-tailed Mann-Whitney *U,* and/or the 2-tailed Wilcoxon signed-rank test as indicated in the figure legends. A p value <0.05 was considered statistically significant. For single-cell experiments, p values were adjusted for multiple testing by the Bonferroni method (*p <0.05; ***p <0.001).

For further details regarding the materials and methods used, please refer to the CTAT table and supplementary information.

Results
TGR5 fluorescence intensity is reduced in BECs in PSC livers
High TGR5 protein expression was detected within or in close proximity to the apical membrane in BECs of control livers stained with antibodies against TGR5 and cytokeratin-7 (CK-7)(Fig. 1A).[13,16,17] In PSC livers, TGR5 staining was also present in BECs and the subcellular distribution was similar to that observed in controls (Fig. 1A). However, the TGR5 fluorescence staining intensity (FI) in relation to CK-7 FI was reduced to 60.6±6.1% (n = 30) of controls, which were set to 100% (n = 28, p <0.05)(Fig. 1B). CK-7 FI was comparable in all livers analyzed (Fig. S1A). Reduced TGR5 BEC FI was detected in both early (I/II, n = 4, p <0.05) and late stage (III/IV, n = 4, p <0.05) PSC tissue, suggesting that TGR5 protein levels are diminished early in the disease process and remain low during disease progression (Fig. S1B). To explore whether downregulation of TGR5 FI in BECs is a common phenomenon in liver diseases, TGR5 BEC FI was determined in livers from patients with primary biliary cholangitis (PBC), non-alcoholic steatohepatitis (NASH), drug-induced liver injury (DILI) and chronic viral hepatitis (Fig. 1C). No reduction of TGR5 BEC FI was observed in liver tissue from these diseases (Fig. 1D) – suggesting a disease-related/-specific downregulation.

To visualize TGR5 in $CD206^+$-macrophages, previously described to be enriched in PSC livers, we counterstained liver tissue with anti-TGR5 and anti-CD206 antibodies.[33] In line with previous findings, TGR5 FI was strong in $CD206^+$-macrophages in PSC tissue, indicating a cell type-specific regulation of TGR5-expression in PSC (Fig. S1C).[33]

Tgr5-expression levels are reduced in intra- and extrahepatic ducts of *Abcb4*$^{-/-}$ mice
To determine whether downregulation of Tgr5 is found in BECs from both intrahepatic and extrahepatic ducts, *Abcb4*$^{-/-}$ mice were used as a model for sclerosing cholangitis. $EpCAM^+/CD30^-/CD45^-/CD11b^-$ BECs were enriched by FACS from livers of 6–8-week-old WT and *Abcb4*$^{-/-}$ mice (Fig. S2A). Relative *Tgr5* mRNA levels were reduced to 43.9±0.7% in $EpCAM^+$-cells derived from *Abcb4*$^{-/-}$ animals compared to WT cells (n = 5 per genotype, p <0.05, Fig. 2A). In contrast, *Tgr5* mRNA expression was unaltered in $EpCAM^-$ non-parenchymal cells from *Abcb4*$^{-/-}$ mice (Fig. S2B). Analysis of micro-dissected intrahepatic lobular ducts (n = 5 *Abcb4*$^{-/-}$, n = 10 WT) or extrahepatic ducts (n = 7 *Abcb4*$^{-/-}$, n = 5 WT) from *Abcb4*$^{-/-}$ animals revealed a significant reduction of *Tgr5* mRNA levels of about 40% and 50%, respectively, compared to WT littermates (Fig. 2B,C).

In contrast, no difference in *Tgr5* mRNA expression was observed in BECs derived from *Abcb4*$^{-/-}$ and WT mice using the micro-dissection and outgrowth method (BECs were cultured for 4–8 passages before analysis) (Fig. S2C).[15,17] Thus, the reduction of Tgr5-expression appears to be a consequence of changes in the livers of *Abcb4*$^{-/-}$ mice rather than of a direct, cell-intrinsic effect of the genetic modification.

To study alterations of Tgr5 on the protein level, immunofluorescence staining was performed on WT and *Abcb4*$^{-/-}$ liver tissue. Immunolocalization detected Tgr5 in the apical membrane domain and also some intracellular vesicular structures of intrahepatic and extrahepatic bile ducts in both WT and *Abcb4*$^{-/-}$ mice (Fig. 2D,F). The FI of Tgr5 in relation to Ck-7 was significantly reduced to 39.0±5.9% in intrahepatic BECs of *Abcb4*$^{-/-}$ compared to WT animals (set to 100%, n = 6 per genotype, p <0.01, Fig. 2E). In extrahepatic BECs, Tgr5 FI was reduced to 46.7±4.3% in *Abcb4*$^{-/-}$ animals (WT set to 100%, n = 3-5 per genotype, p <0.05, Fig. 2F). Ck-7 FI was similar between genotypes (Fig. S3A). Counterstaining of Tgr5 and macrophages with anti-Tgr5, anti-F4/80 and anti-CD68 antibodies revealed a strong Tgr5 fluorescence signal in both $F4/80^+$ and $CD68^+$ intrahepatic macrophages, especially in *Abcb4*$^{-/-}$ livers (Fig. S3B). This finding is in line with the 3.1-fold increase of *Tgr5* mRNA expression in whole liver tissue from *Abcb4*$^{-/-}$ mice compared to WT (n = 12 per genotype, p <0.05), emphasizing that the downregulation of Tgr5 in BECs is cell type specific (Fig. S3C).

Interleukin-8 (CXCL-8) and its murine homologues suppress TGR5 levels in murine and human cholangiocytes
Increased senescence has been identified as a hallmark of PSC and cholangiocytes derived from PSC livers express and secrete inflammatory cytokines and chemokines such as interleukin (IL) 6, IL8 (CXCL8) and CC-chemokine ligand-2 (CCL2), which are markers of the senescence-associated secretory phenotype.[6,34,35,36] High levels of IL8 in the bile and serum of patients with PSC are associated with disease progression and reduced transplant-free survival.[37,38] Therefore, we tested whether Il8 homologues, Il6 and Ccl2 are increased in serum from 6–8-week-old *Abcb4*$^{-/-}$ mice. Indeed, serum levels for KC/Cxcl1, Mip2/Cxcl2, Il6, Ccl4 and Ccl2 were elevated by 1.8-, 1.2-, 2.5-, 1.4- and 1.7-fold in *Abcb4*$^{-/-}$ mice compared to WT littermates (n = 22 *Abcb4*$^{-/-}$, n = 13 WT, Fig. 3A, Fig. S4). In contrast, serum levels of Il1β, tumor necrosis factor (Tnf)-α and Il10 were similar in both genotypes (Fig. S4).

Given the potential role of IL8 as a promotor of disease progression, we incubated primary murine BECs for 24 h with Cxcl1/Cxcl2. Cxcl1 and to a lesser extent Cxcl2 suppressed relative *TGR5* mRNA levels to 61.1±8.0% and 76.7±9.2%, respectively, compared to vehicle-treated controls (n = 7-8, p <0.05, Fig. 3B). In contrast, incubation with Tnfα, Il6, Il1β and Ccl4 did not affect *Tgr5* mRNA levels (n = 7-27 each, Fig. 3B). Pre-treatment with reparixin, an

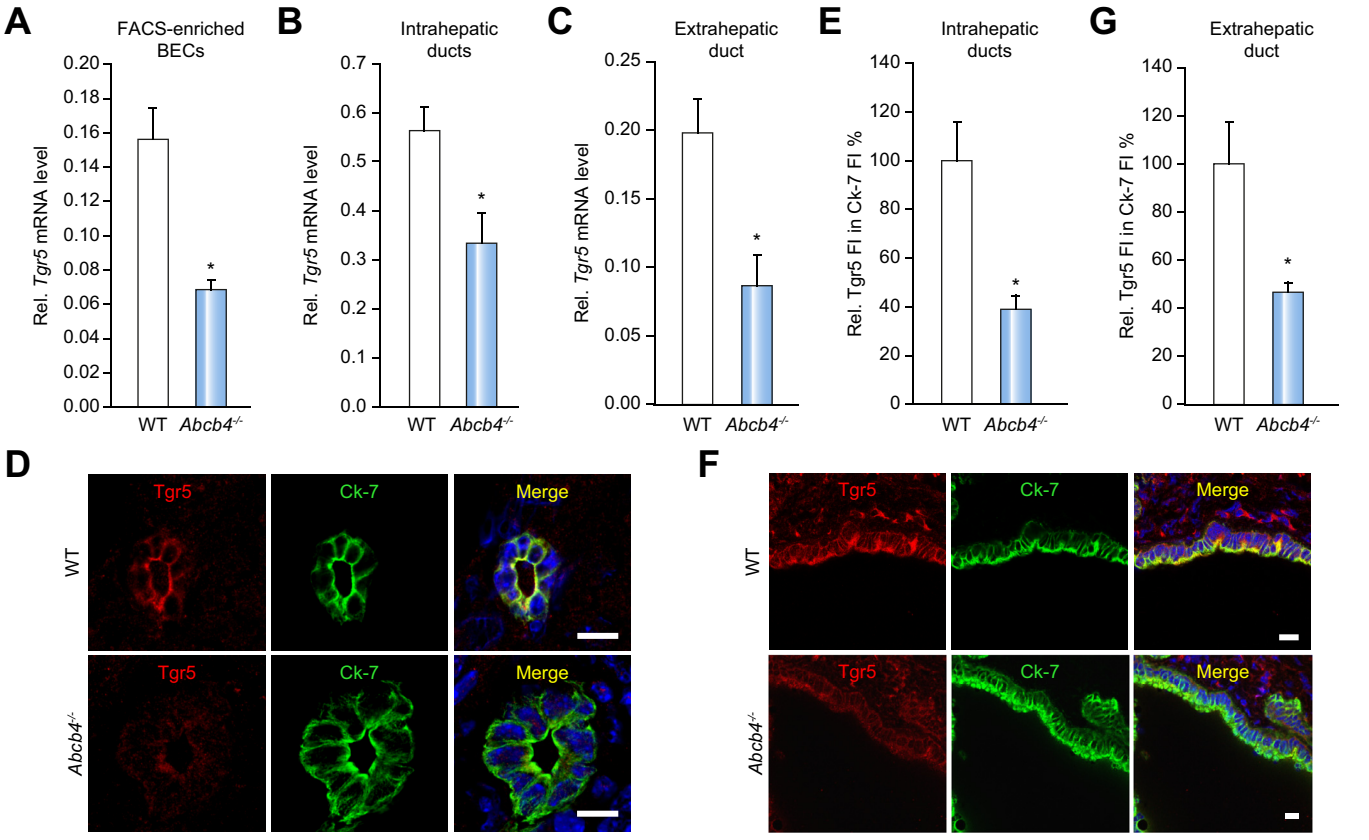

Fig. 2. Tgr5 levels are reduced in the biliary tree of *Abcb4*$^{-/-}$ mice. (A) *Tgr5* mRNA was measured in relation to Hprt1 in FACS-enriched BECs (n = 5). (B) *Tgr5* mRNA was determined in relation to Hprt1 in micro-dissected intrahepatic bile ducts from *Abcb4*$^{-/-}$ and WT animals (n = 5-10). (C) *Tgr5* mRNA was measured in relation to Hprt1 in the extrahepatic bile ducts from *Abcb4*$^{-/-}$ and WT mice (n = 5-7). (D) Frozen liver sections were double-labelled for Tgr5 (red) and Ck-7 (green). (E) Relative Tgr5 FI was determined in relation to Ck-7 FI (n = 6 each, WT set to 100%). (F) Frozen sections of extrahepatic bile ducts from WT and *Abcb4*$^{-/-}$ were double-labelled for Tgr5 (red) and Ck-7 (green). (G) Tgr5 FI is depicted in relation to Ck-7 FI (n = 5 WT, n = 3 *Abcb4*$^{-/-}$, WT = 100%). Data are shown as mean ± SEM; *significantly different to WT livers or WT BECs/ducts (p <0.05 as determined by Mann-Whitney U test). Nuclei are shown in blue. Bars = 10 μm. BECs, biliary epithelial cells; FI, fluorescence intensity; WT, wild-type.

allosteric inhibitor of the CXC chemokine receptors 1/2 (Cxcr1/2) attenuated the Cxcl1-induced downregulation of Tgr5-expression (Fig. S5A).

To test whether these results could be transferred to human disease, BECs were isolated from human liver and stimulated with IL8 for 24 h. A significant reduction of relative TGR5 protein levels to 71.1±11.9% of vehicle-treated controls was detected by western blotting (n = 8 each, p <0.05, Fig. 3C,D). Furthermore, we derived organoids from human bile.[27] Bile-derived organoids expressed biliary markers such as CK-19, CK-7 and SOX9, and showed absent or only low expression levels of hepatocyte genes, such as albumin and hepatocyte nuclear factor 4α (Fig. 3E, Fig. S6).[27] Stimulation of bile-derived organoids with IL8 for 24 h significantly reduced *TGR5* mRNA expression to 67.1±4.9% of vehicle-treated controls (n = 4, p <0.05, Fig. 3F), which was abrogated in the presence of a CXCR1/2 inhibitor (Fig. S5B).

To explore whether TGR5-expression is also downregulated in the setting of senescence-associated paracrine biliary injury, we stained Tgr5 and Ck-19 in liver tissue from mice, which develop biliary senescence based on the conditional deletion of murine double minute-2 (*Mdm2*) under the control of the Ck-19 promotor.[36] Relative Tgr5 FI in relation to Ck-19 FI was significantly reduced in these animals 8 and 11 days after the induction of biliary senescence (Fig. S7).

Taken together, these data strongly suggest that downregulation of TGR5 in murine and human BECs may occur in response to biliary senescence and paracrine secretion of IL8 and its homologues.

Reduced Tgr5 levels are associated with decreased Tgr5 signaling in BECs and predispose to more severe biliary injury

To investigate whether Tgr5 downregulation affects Tgr5-dependent signaling, BECs isolated from WT and *Abcb4*$^{-/-}$ livers were subjected to western blotting for extracellular signal-regulated kinase (Erk)1/2 phosphorylation and total Erk1/2. In line with reduced Tgr5 protein levels, Erk1/2 phosphorylation was lower in BECs derived from *Abcb4*$^{-/-}$ livers (n = 6 WT, n = 9 *Abcb4*$^{-/-}$, p <0.05, Fig. 4A). The same result was obtained when whole liver samples were analyzed (n = 4 per genotype, p <0.05, Fig. 4B). Since Tgr5 levels in BECs were reduced by about 40–60% in this study, we investigated whether deletion of Tgr5 on only 1 allele would suffice to render mice more susceptible to biliary injury after LCA feeding. WT, *Tgr5*$^{+/-}$ and *Tgr5*$^{-/-}$ mice were fed LCA (1%) over 84 h, which resulted in severe liver damage in all genotypes.[7,8,39] Analysis of the biliary phenotypes revealed that heterozygous *Tgr5*$^{+/-}$ animals developed significantly higher serum alkaline phosphatase (ALP) levels and an aggravated

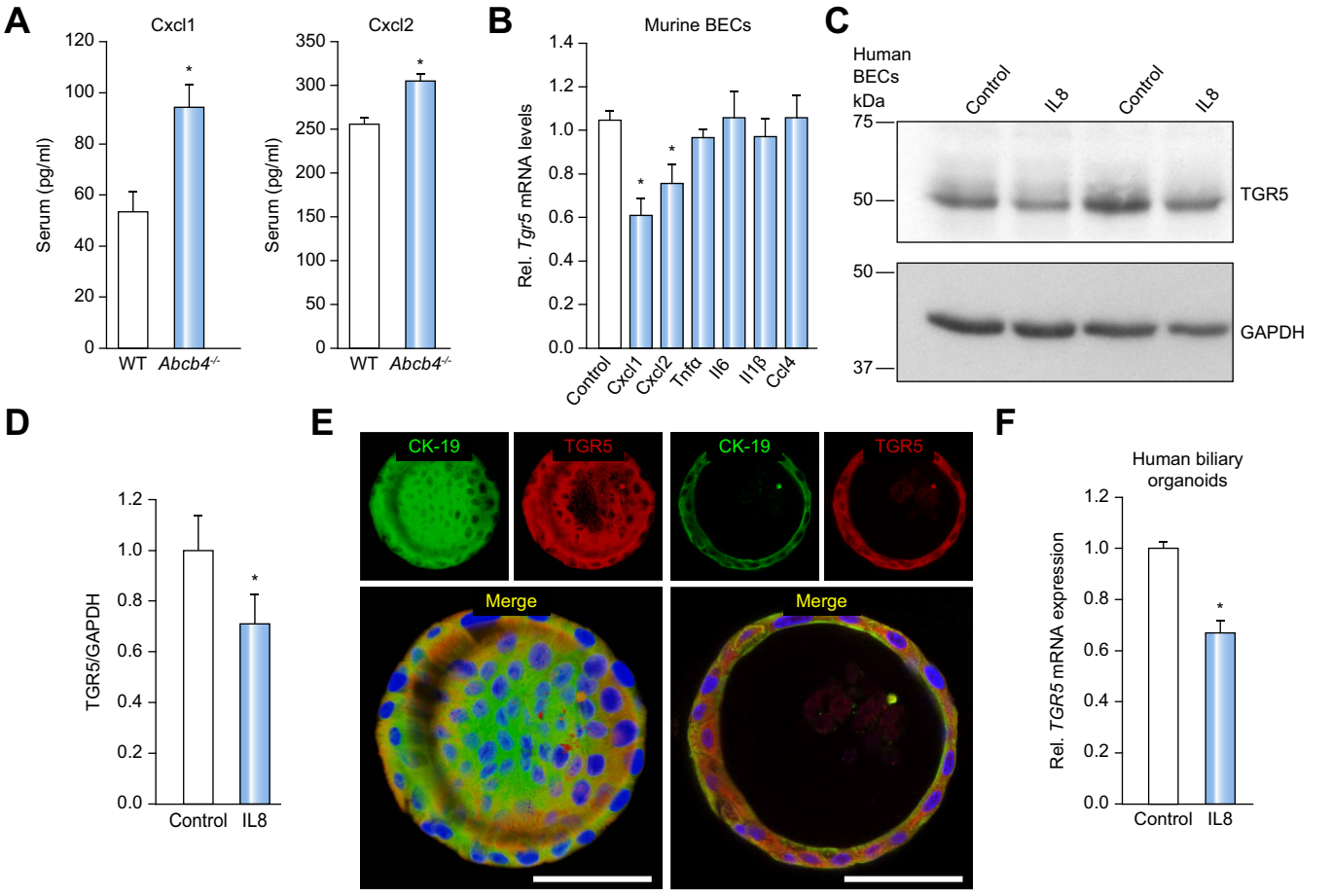

Fig. 3. Treatment of murine and human BECs with IL8 and its homologues triggers a reduction in TGR5 mRNA and protein levels. (A) Serum levels of Cxcl1/2 were measured in 6–8-week-old WT and *Abcb4*$^{-/-}$ mice (n = 13 WT, n = 22 *Abcb4*$^{-/-}$). (B) Murine BECs were incubated with Cxcl1 and Cxcl2 (200 ng/ml), Tnfα (5 ng/ml), Il6 (20 ng/ml), Il1β (2 ng/ml) and Ccl4 (10 ng/ml) for 24 h. *Tgr5* mRNA expression was analyzed in relation to Gapdh (n = 7-27 per condition). (C) Human BECs were isolated from patients with alcohol-related liver disease or NAFLD. Cells were stimulated with IL8 (5 ng/ml) for 24 h. Cell lysates were separated by SDS-page, blotted onto PVDF membranes, and detection was carried out using anti-TGR5 and anti-GAPDH antibodies. (D) TGR5 and GAPDH protein amounts were quantified by densitometric analysis. The values for untreated cells (control) were set to 1.0 (n = 8 per condition). (E) Bile-derived human biliary organoids were stained with antibodies against CK-19 and TGR5. Left panel: Partial 3D-reconstruction of a bile-derived biliary organoid. Nuclei were stained with Hoechst, Bars = 50 μm. Right panel: Plane taken from a single Z-stack plane. (F) Stimulation of bile-derived human organoids with IL8 for 24 h resulted in a significant reduction of *TGR5* mRNA expression in relation to GAPDH (n = 4). Data are expressed as mean ± SEM; *significantly different to WT/vehicle-treated controls (p <0.05, Mann-Whitney *U* test/Wilcoxon signed-rank test). BECs, biliary epithelial cells; NAFLD, non-alcoholic fatty liver disease; PVDF, polyvinylidene fluoride; WT, wild-type.

sclerosing cholangitis phenotype on histology as compared to WT littermates (Fig. S8).

Single-cell RNA-sequencing reveals intrahepatic cholangiocytes from *Abcb4*$^{-/-}$ mice have an activated, inflammatory phenotype

EpCAM^{+}-BECs were sorted from liver cell lysates by FACS prior to single-cell RNA-sequencing (scRNA-seq) analysis using 10x Genomics. After filtering, a total of 40,333 cells from 8 livers (n = 4 per genotype) were used for further analysis. UMAP projection of the clustering revealed 9 clusters which were assigned to cell types using known lineage markers (Fig. 5A).[40] The sequencing data for this project can be accessed on GEO (accession number GSE168758). BECs were characterized by expression of EpCAM, Sox9, Spp1, Krt7 (Ck-7), Krt19 (Ck-19), Tm4sf4 and clusterin (Fig. S9B).[41,42] In line with increased ductular reaction, a larger number of EpCAM^{+}-BECs were derived from *Abcb4*$^{-/-}$ livers (Fig. 5B). While Tgr5 was detected in BECs, Tgr5-expression levels were low, which is in line with previous findings, therefore clustering according to Tgr5-expression levels was not pursued.[41,43] Comparison of WT and *Abcb4*$^{-/-}$ BECs revealed a significant upregulation of genes previously associated with an activated ("reactive") inflammatory BEC phenotype, such as intercellular adhesion molecule-1 (Icam1), vascular cellular adhesion molecule (Vcam1), Ccl2 and transforming growth factor-β2 (Tgfβ2) (Fig. 5C).[44,45] 307 genes were differentially regulated between WT and *Abcb4*$^{-/-}$ BECs (Fig. 5D). Pathway analysis revealed an activation of NF-κB, Toll-like receptor (Tlr)2, Il6 and Il17A signaling in *Abcb4*$^{-/-}$ BECs (Fig. 5E).

Tgr5 overexpression improves sclerosing cholangitis in *Abcb4*$^{-/-}$ mice

To investigate the link between reduced Tgr5-expression and the reactive biliary phenotype, we crossed *Abcb4*$^{-/-}$ mice with Tgr5-overexpressing transgenic mice (*Tgr5*^{Tg})[25] and compared these *Abcb4*$^{-/-}$/*Tgr5*^{Tg} to *Abcb4*$^{-/-}$/*Tgr5*^{WT} littermates. Tgr5 FI in intrahepatic BECs from *Abcb4*$^{-/-}$/*Tgr5*^{Tg} mice was significantly higher than in those from *Abcb4*$^{-/-}$/*Tgr5*^{WT} mice (Fig. 6A), which was in

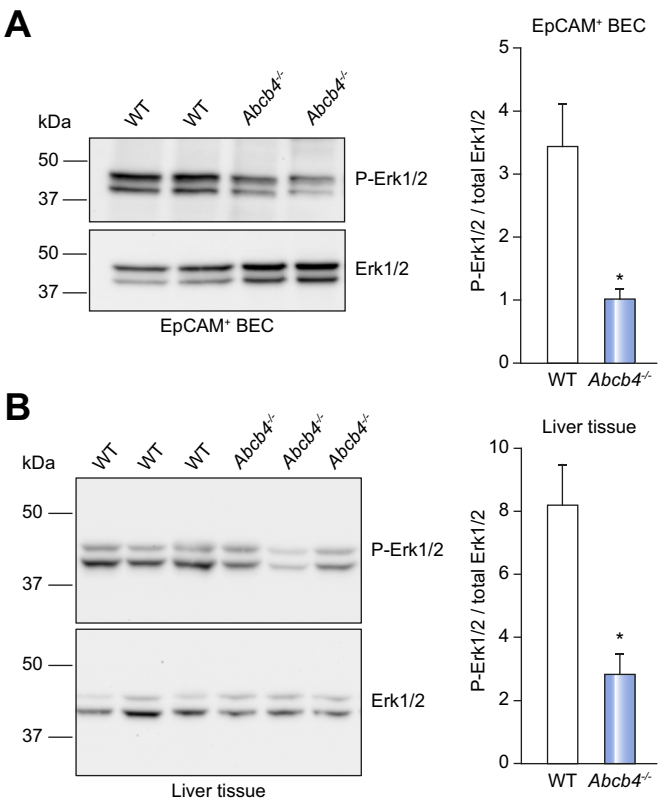

Fig. 4. Erk1/2 phosphorylation is reduced in cholangiocytes and liver tissue of *Abcb4*$^{-/-}$ mice. Western blot analysis of phosphorylated Erk1/Erk2 and total Erk1/2 were carried out in (A) primary, FACS-sorted BECs from WT (n = 6) and *Abcb4*$^{-/-}$ (n = 9) mice, and in (B) liver lysates from *Abcb4*$^{-/-}$ and WT mice (n = 4 per genotype). Phosphorylated Erk1/2 *vs.* total amount of Erk1/2 was determined by densitometric analysis. Data are expressed as mean ± SEM, *significant difference (p <0.05, Mann-Whitney U test). BECs, biliary epithelial cells; WT, wild-type.

line with increased *Tgr5* mRNA levels in both intra- and extrahepatic BECs of *Tgr5*^{Tg} mice (Fig. 6B, Fig. S10A). *Abcb4*$^{-/-}$/*Tgr5*^{Tg} mice developed a less severe sclerosing cholangitis phenotype as demonstrated by improved liver histology (Fig. 6C) and reduced levels of aspartate aminotransferase, alanine aminotransferase and ALP (Fig. 6D, Fig. S10B). Serum levels of Cxcl1 and Cxcl2 were significantly lower in *Abcb4*$^{-/-}$/*Tgr5*^{Tg} mice (Fig. 6D). Hepatic *Ck*-19 mRNA levels were diminished in *Abcb4*$^{-/-}$/*Tgr5*$^{Tg+}$ livers, indicating a reduced ductular reaction (Fig. 6E, Fig. S10C). Enhanced Tgr5-expression led to a significant reduction in hepatic expression of collagen-1α1, Ccl2 and Tnfα, while levels for Tgfβ2 and Icam1 were significantly lowered to levels observed in WT animals (Fig. 6E, Fig. S10D).

To investigate whether Tgr5 overexpression also improves the inflammatory BEC phenotype, scRNA-seq was performed (Fig. 7A). There was a significant reduction in expression of *Icam1, Vcam1* and *Cxcl1* in BECs from *Abcb4*$^{-/-}$/*Tgr5*^{Tg} mice compared to *Abcb4*$^{-/-}$/*Tgr5*^{WT}(n = 4 each, Fig. 7C). Overall, 46 genes were differentially regulated in BECs from these animals (Fig. 7D). Pathway analysis revealed an inhibition of IκBκB, Tlr3, Tnfα, Il17A and Il1α signaling pathways in *Abcb4*$^{-/-}$/*Tgr5*^{Tg} compared to *Abcb4*$^{-/-}$/*Tgr5*^{WT} (Fig. 7E). These findings suggest that enhanced Tgr5-expression and signaling attenuates development of a reactive BEC phenotype.

NorUDCA restores Tgr5 levels in BECs of *Abcb4*$^{-/-}$ mice

NorUDCA has been shown to improve the sclerosing cholangitis phenotype of *Abcb4*$^{-/-}$ mice and to lower ALP serum levels in patients with PSC.[45,46] Therefore, we analyzed Tgr5 FI in livers of *Abcb4*$^{-/-}$ mice fed for 4 weeks with norUDCA or UDCA as described.[45] Tgr5 FI in BECs of norUDCA-fed *Abcb4*$^{-/-}$ animals was increased by 3.2-fold compared to untreated mice and thus restored to levels comparable to WT animals (Fig. 8A,B). UDCA-feeding led to a significant increase in *Tgr5* mRNA levels, but only partially restored Tgr5 FI in relation to WT levels. Addition of norUDCA or UDCA for 24 h to murine BECs, which were pre-incubated with Cxcl1 for 24 h, reversed the Cxcl1-induced downregulation of *Tgr5* mRNA levels (Fig. 8C). Similarly, norUDCA restored IL8-induced downregulation of *TGR5* mRNA levels in human bile-derived organoids (Fig. 8D).

Discussion

Chronic inflammation, cholestasis and fibrosis are the hallmarks of PSC. The initial trigger of the disease is still unknown and may differ between patient populations.[1,2] It has been speculated that exposure of the biliary epithelium to pathogens or microbial-derived products in a genetically predisposed individual may trigger the development of an activated, pro-inflammatory BEC phenotype, which is found in PSC as well as *Abcb4*$^{-/-}$ animals.[1,2,5,6]

Since TGR5 is highly expressed in BECs and exerts protective effects,[13,17,22] we evaluated changes in TGR5-expression, localization and signaling in livers from patients with PSC and *Abcb4*$^{-/-}$ animals.[4,7] Assessment of liver tissue from different liver diseases (PSC, PBC, NASH, DILI, viral hepatitis) demonstrated a significant downregulation of TGR5 only in BECs from PSC livers. This downregulation was present in the early stages of disease and persisted throughout disease progression. The reduction of TGR5 FI was not observed in intrahepatic CD206^{+}-macrophages as described previously.[33]

Accordingly, higher *Tgr5* mRNA levels were detected in whole liver tissue of *Abcb4*$^{-/-}$ animals, which may be attributed to accumulation of Tgr5-expressing monocytes/macrophages in livers of *Abcb4*$^{-/-}$ mice.[33,34] In contrast, a significant reduction of *Tgr5* mRNA levels was detected in FACS-isolated BECs (50.6% of WT levels) as well as in micro-dissected intrahepatic (59.3% of WT levels) and extrahepatic ducts (43.8% of WT levels) from *Abcb4*$^{-/-}$ mice. Furthermore, Tgr5 protein levels as measured by immunofluorescence staining were significantly lower in intrahepatic and extrahepatic BECs of *Abcb4*$^{-/-}$ animals, indicating a cell type-specific regulation of Tgr5.

Since no difference in Tgr5-expression was observed between *ex vivo* cultured BECs from *Abcb4*$^{-/-}$ and their WT littermates, we speculated that the reduction of Tgr5-expression in BECs was due to disease-associated changes within the peribiliary microenvironment. Development of a reactive BEC phenotype, which is characterized by increased cell proliferation, expression and secretion of pro-inflammatory cytokines, chemokines and adhesion molecules (*e.g.* Icam1, Vcam1) has been described for PSC.[6,35,44,47] Persistence of biliary injury may then trigger development of BEC senescence, which aggravates and perpetuates biliary injury in a paracrine manner.[6,35,36] Indeed, using scRNA-seq, a significant increase in Icam1-, Vcam1-, Ccl2-and Tgfβ2-expression was detected in BECs from *Abcb4*$^{-/-}$ animals.

High levels of IL8 in the bile and serum of patients with PSC may serve as a prognostic factor and are associated with reduced

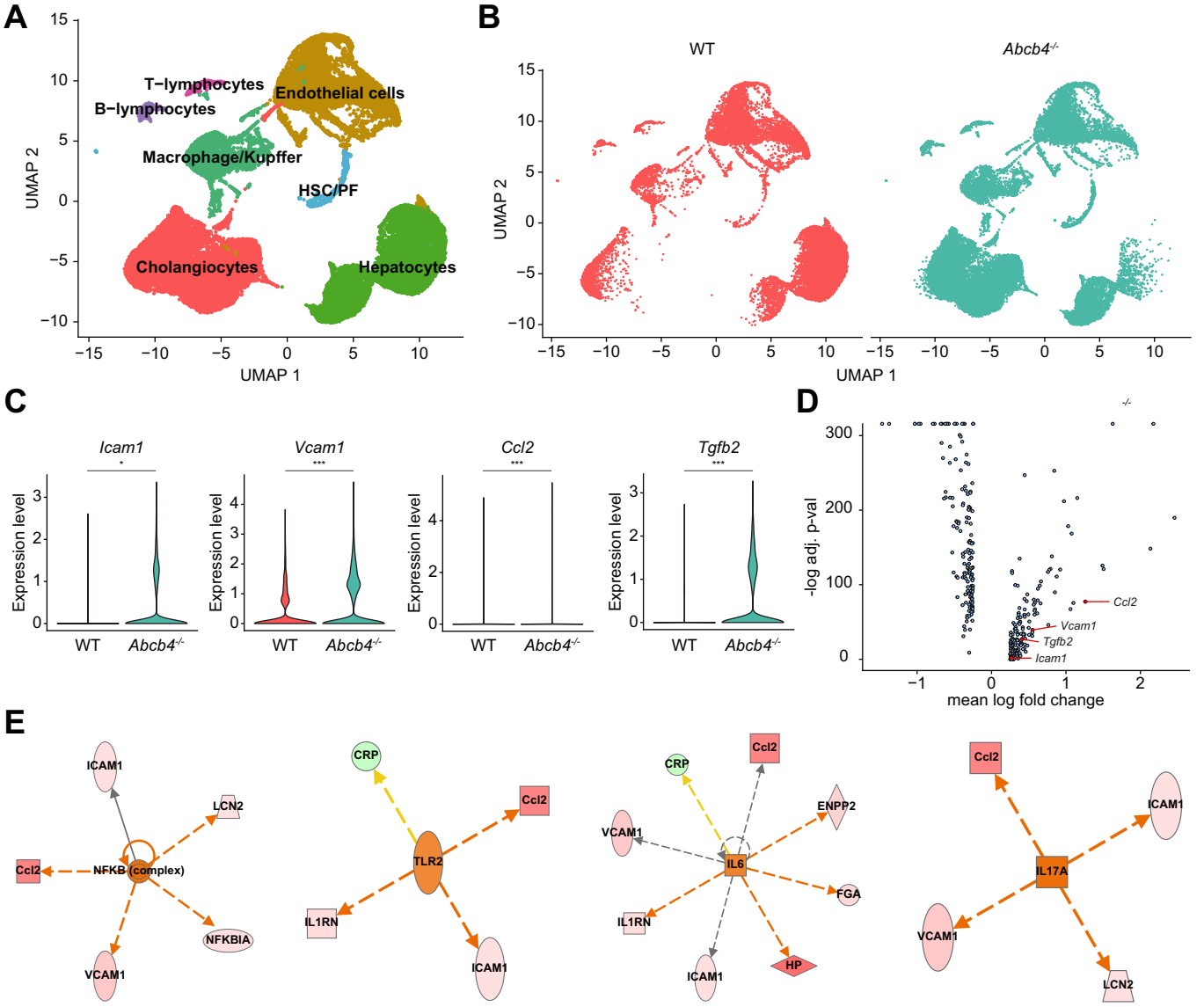

Fig. 5. Single-cell RNA-seq analysis reveals an inflammatory reactive BEC phenotype in *Abcb4*$^{-/-}$ mice. (A) BECs were enriched from whole liver lysates by FACS. UMAP visualization of 40,333 cells from WT and *Abcb4*$^{-/-}$ mice (n = 4 per genotype) showing cell clusters according to their gene expression. (B) Clustering according to genotype. (C) Violin plots showing gene expression in BECs from WT and *Abcb4*$^{-/-}$ mice. (D) Differentially expressed genes (n = 307) between WT and *Abcb4*$^{-/-}$ mice. (E) Pathway analysis using IPA-software, which is based on the expression levels of downstream targets, as measured by scRNA-seq. Activation is depicted in orange, inhibition in blue, increased expression in pink and decreased expression in green. *p* values were determined by the Wilcoxon rank sum test and adjusted for multiple testing by the Bonferroni method. **p* <0.05; ****p* <0.001. BECs, biliary epithelial cells; IPA, Ingenuity Pathway Analysis; scRNA-seq, single-cell RNA-sequencing; UMAP, uniform manifold approximation and projection; WT, wild-type.

transplant-free survival.[37] IL8 acts as a neutrophil chemoattractant and activator, and is upregulated early after biliary injury in PSC and also in biliary atresia.[37,38,48,49] We therefore tested whether IL8 modulates TGR5-expression. Stimulation of murine and human BECs with IL8/Il8 homologues resulted in decreased *TGR5* mRNA and protein levels, respectively. This was not observed in murine BECs in response to Tnfα, Il6, Il1β and Ccl4 or in cells/organoids pretreated with a Cxcr1/2 inhibitor. However, we cannot rule out that further factors, such as biliary senescence or other paracrine factors contribute to the down-regulation of Tgr5. To investigate whether the observed reduction in Tgr5 levels is sufficient to affect Tgr5-signaling and thus cytoprotective mechanisms in BECs, Erk1/2 phosphorylation was analyzed in FACS-isolated BECs. In line with the reduced Tgr5-levels, lower Erk1/2 phosphorylation was detected, although factors independent of Tgr5 may contribute to the reduced Erk1/2 activation. Another downstream effect of Tgr5 in BECs is cell proliferation. While BECs derived from *Tgr5*$^{-/-}$ mice show no proliferation in response to BAs, cell proliferation induced by cytokines/chemokines is unaltered (Fig. S12). Since cytokine/chemokine levels are significantly elevated in *Abcb4*$^{-/-}$ mice, cholangiocyte proliferation can be triggered independently of Tgr5. The protective effect of Tgr5 in BECs, against the toxic effects of BA, was analyzed in heterozygous Tgr5-deficient mice, which were challenged by LCA.[4,39] Tgr5 heterozygous animals developed a severe

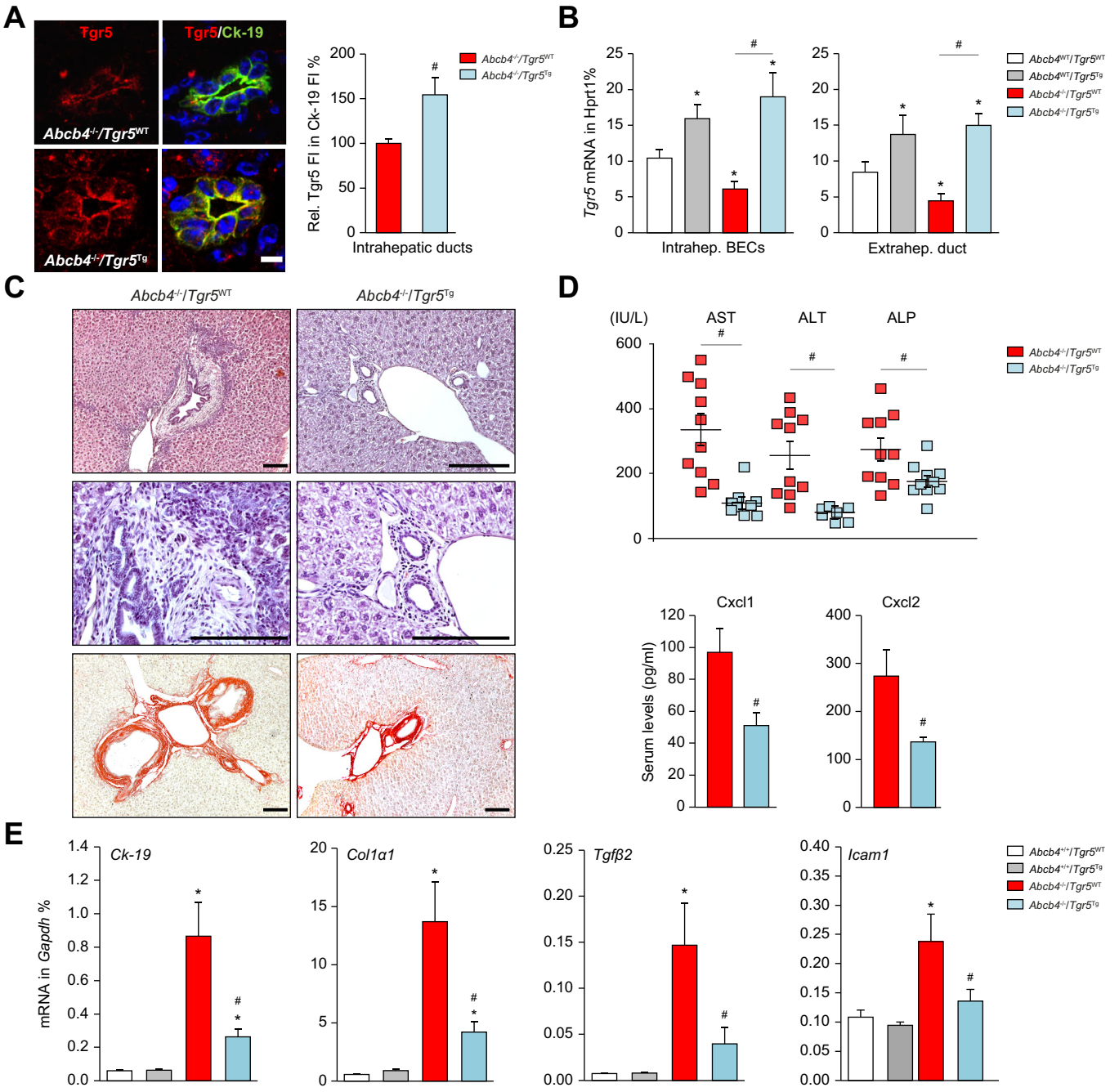

Fig. 6. Sclerosing cholangitis in *Abcb4*$^{-/-}$ mice is improved by overexpression of Tgr5. (A) Liver sections from 6–8-week-old *Abcb4*$^{-/-}$/*Tgr5*^{WT} and *Abcb4*$^{-/-}$/*Tgr5*^{Tg} were double-labelled for Tgr5 (red) and Ck-19 (green). Nuclei shown in blue, bars = 10 μm. Relative Tgr5 FI was determined in bile ducts in relation to Ck-7 FI (n = 5 per genotype). Relative Tgr5 FI in *Abcb4*$^{-/-}$/*Tgr5*^{WT} animals was set to 100%. (B) *Tgr5* mRNA was measured in relation to Hprt1 in FACS-enriched BECs (n = 5-7 per genotype) and micro-dissected extrahepatic ducts (n = 7–19 per genotype) (C) H&E and Sirius red staining of liver tissue from *Abcb4*$^{-/-}$/*Tgr5*^{WT} and *Abcb4*$^{-/-}$/*Tgr5*^{Tg}. Bars = 100 μm. (D) Serum levels for AST, ALT, ALP, Cxcl1 and Cxcl2 (n = 8–10 per genotype). (E) Analysis of mRNA levels in whole liver tissue for *Ck-19*, *collagen1α1*, *Tgfβ2* and *Icam1* in relation to Gapdh (n = 7-12 per genotype). Data are expressed as mean ± SEM; *significant difference to *Abcb4*$^{+/+}$/*Tgr5*^{WT}; #significant difference to *Abcb4*$^{-/-}$/*Tgr5*^{WT} (p <0.05, Mann-Whitney *U* test). BECs, biliary epithelial cells; FI, fluorescence intensity; WT, wild-type.

cholangitis phenotype, supporting the hypothesis that a reduction of Tgr5 protein levels is sufficient to render both intra- and extrahepatic BECs more susceptible to cellular injury. In contrast, overexpression of Tgr5 in *Abcb4*$^{-/-}$ mice improved sclerosing cholangitis and ameliorated the reactive BEC phenotype, as demonstrated by reduced expression of Icam1, Vcam1 and Cxcl1 and inhibition of inflammatory pathways. These data underscore that enhanced Tgr5-expression and signaling may prevent development of an inflammatory, reactive BEC phenotype. Indeed, sclerosing cholangitis in *Abcb4*$^{-/-}$ mice was improved by administration of a dual TGR5/FXR agonist (INT-767)[50] and can be cured by norUDCA-feeding.[45] *In vitro*, norUDCA, tauro-norUDCA and UDCA completely restored *TGR5* mRNA levels in Cxcl1/IL8-treated murine/human

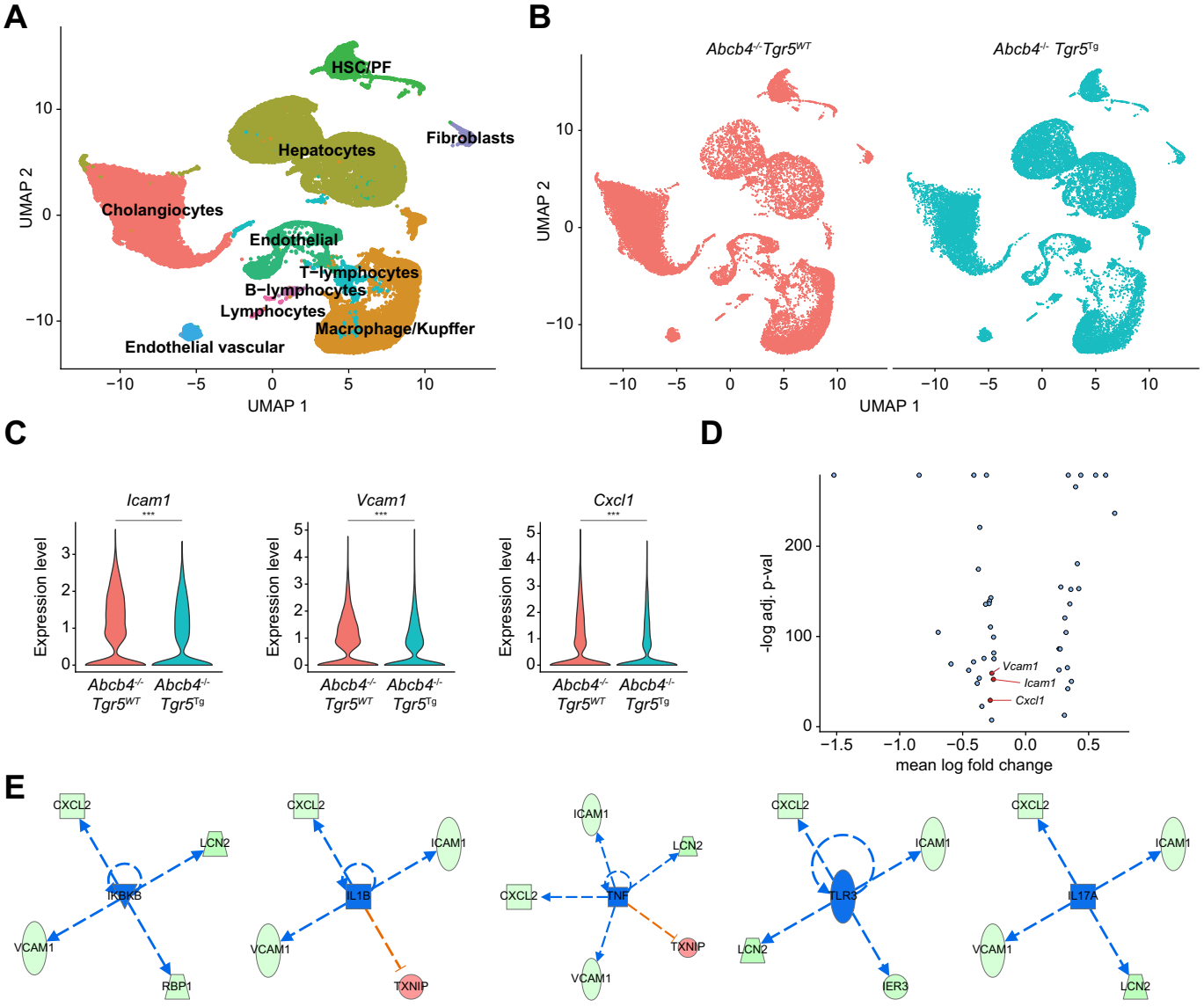

Fig. 7. Overexpression of Tgr5 ameliorates the reactive BEC phenotype in *Abcb4*$^{-/-}$ mice. (A) Intrahepatic BECs were enriched by FACS prior to scRNA-seq. Clustering of 47,764 cells from *Abcb4*$^{-/-}$*Tgr5*^{WT} (denoted as *Abcb4*$^{-/-}$) and *Abcb4*$^{-/-}$*Tgr5*^{Tg} mice (n = 4 per genotype) using expression of marker gene signatures, and (B) clustering according to genotype. (C) Violin plots showing gene expression in BECs from *Abcb4*$^{-/-}$*Tgr5*^{WT} and *Abcb4*$^{-/-}$*Tgr5*^{Tg} (n = 4 per genotype). (D) Differentially expressed genes (n = 46) between *Abcb4*$^{-/-}$*Tgr5*^{WT} and *Abcb4*$^{-/-}$*Tgr5*^{Tg}. (E) Pathway analysis as predicted by IPA-software. Inhibition is depicted in blue, increased expression in pink and decreased expression in green. *p* values determined by the Wilcoxon rank sum test and adjusted for multiple testing by the Bonferroni method. ***p <0.001. BECs, biliary epithelial cells; IPA, Ingenuity Pathway Analysis; scRNA-seq, single-cell RNA-sequencing; WT, wild-type.

BECs. *In vivo*, UDCA-feeding resulted in significantly higher Tgr5 levels in BECs, however these did not reach WT levels. In contrast, Tgr5 FI in BECs was restored to WT levels after norUDCA treatment. It is possible that due to the presence of cholehepatic shunting *in vivo*, norUDCA reaches higher biliary concentrations than UDCA or tauro-norUDCA.[51] Both norUDCA and UDCA exert anti-inflammatory effects, which may contribute to the upregulation of biliary Tgr5 levels in *Abcb4*$^{-/-}$ mice.[52] Enhanced biliary Tgr5-expression may then amplify the norUDCA-dependent increase in biliary bicarbonate secretion.[51]

Taken together, the downregulation of biliary TGR5-expression seen in PSC and Abcb4-deficient mice contributes to the development of an inflammatory reactive BEC phenotype. This can be attenuated in *Abcb4*$^{-/-}$ mice by overexpression of Tgr5 or restoration of Tgr5 levels by norUDCA. Preservation and upregulation of TGR5-expression may be a hitherto undescribed mechanism of norUDCA activity and upregulation of TGR5 levels may therefore prove beneficial in PSC.

Abbreviations

Abcb4, ABC binding cassette transporter B4; ALP, alkaline phosphatase; BA, bile acid; BEC, biliary epithelial cell (= cholangiocyte); CCL, CC-chemokine ligand; CK-19, cytokeratin-19 (=Krt19); CK-7, cytokeratin-7 (=Krt7); CXCL, CXC chemokine ligand; DILI, drug-induced liver injury; EpCAM, epithelial cell adhesion molecule; ERK, extracellular signal-regulated kinases; FI, fluorescence intensity; Icam1, intracellular adhesion

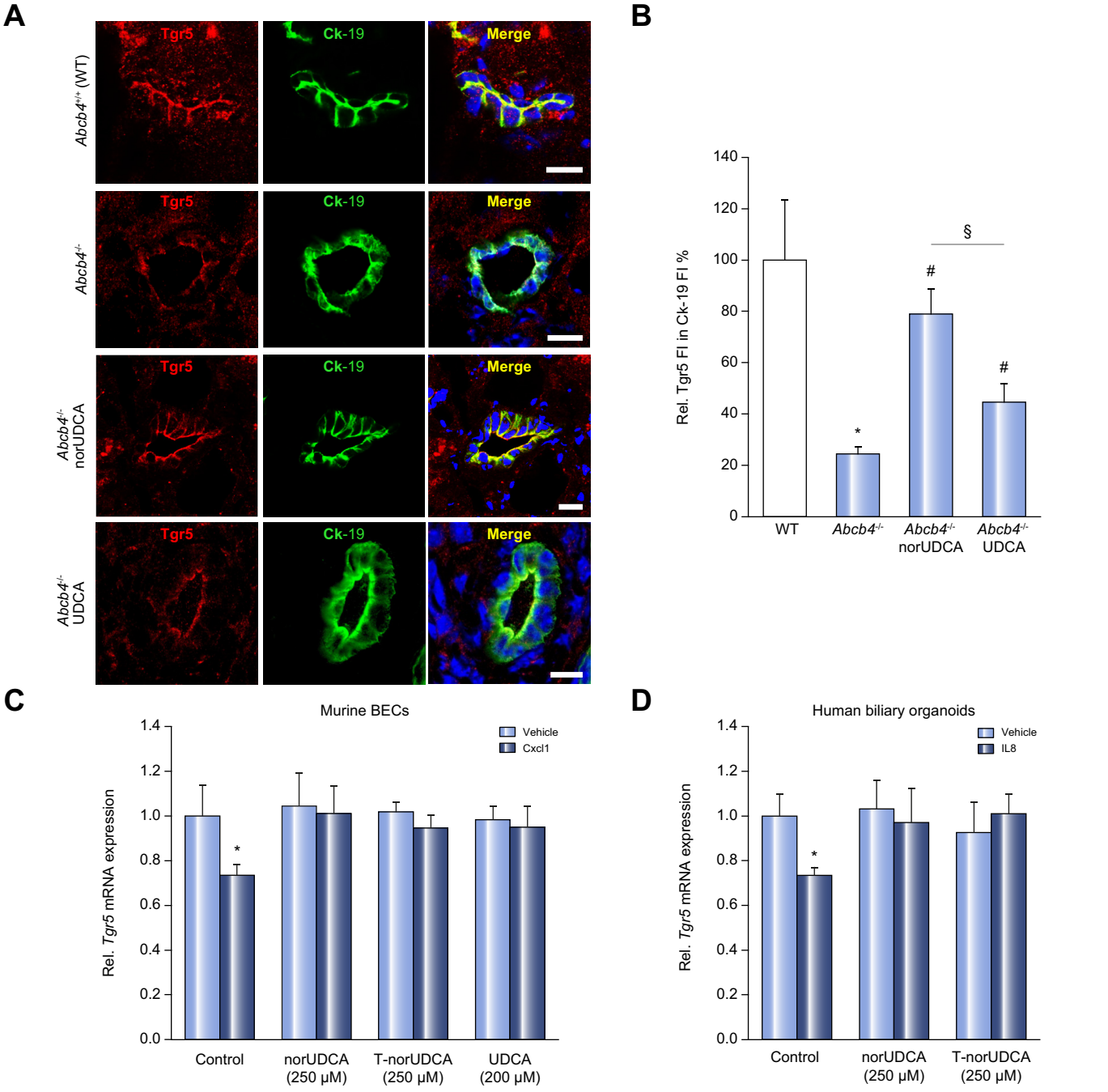

Fig. 8. NorUDCA restores Tgr5 FI in BECs of *Abcb4*$^{-/-}$ animals. (A) Liver sections from 6–8-week-old *Abcb4*$^{+/+}$(=WT), *Abcb4*$^{-/-}$ and *Abcb4*$^{-/-}$ mice fed a diet enriched with norUDCA or UDCA (0.5% each) for 4 weeks were double-labelled for Tgr5 (red) and Ck-19 (green). Nuclei were stained with Hoechst. Bars = 10 µm. (B) Relative Tgr5 FI was determined in BECs in relation to Ck-19 FI (n = 5-7 per genotype/condition). Relative Tgr5 FI in WT animals was set to 100%. *significantly different from WT livers; #significantly different from *Abcb4*$^{-/-}$ mice; §significantly different from norUDCA-treated *Abcb4*$^{-/-}$ mice (p <0.05, Mann-Whitney U test). (C) Primary murine BECs were pretreated with Cxcl1 or vehicle for 24 h and subsequently incubated with norUDCA (250 µM), tauro-norUDCA (250 µM) or UDCA (200 µM) for another 24 h. *Tgr5* mRNA expression was determined in relation to Hprt1 (n = 5-8). (D) Human bile-derived organoids were pretreated with IL8 or vehicle for 24 h and subsequently incubated with norUDCA (250 µM) or tauro-norUDCA (250 µM) for another 24 h. *TGR5* mRNA expression was determined in relation to *HPRT1* (n = 5-9). Data are shown as mean ± SEM; *significantly different from vehicle-treated BECs (p <0.05, Wilcoxon signed-rank test). BECs, biliary epithelial cells; FI, fluorescence intensity; norUDCA, 24-norursodeoxycholic acid; UDCA, ursodeoxycholic acid; WT, wild-type.

molecule-1; IL, interleukin; KC, keratinocyte-derived cytokine/cytokine-induced neutrophil-attracting chemokine (=Cxcl1); LCA, lithocholic acid; Mdr2, multidrug resistance-associated protein-2 (Abcb4); MIP2, macrophage inflammatory protein 2 (=Cxcl2); NASH, non-alcoholic steatohepatitis; norUDCA, 24-norursodeoxycholic acid; PBC, primary biliary cholangitis; PSC, primary sclerosing cholangitis; ROI, region of interest; scRNA-seq, single-cell RNA-sequencing; Spp1, secreted phosphoprotein-1 (=osteopontin); Tgfβ2, transforming growth factor-β2; TGR5, Takeda G protein-coupled receptor-5 (=G

protein-coupled bile acid receptor-1 [GPBAR1]); $Tgr5^{Tg}$, Tgr5 transgenic/overexpressing; Tlr, toll-like receptor; Tm4sf4, transmembrane 4 superfamily member-4; Tnf, tumor necrosis factor; UDCA, ursodeoxycholic acid; UMAP, uniform manifold approximation and projection; Vcam1, vascular cell adhesion protein-1; WT, wild-type.

Financial support
This work was funded by the German Research Foundation (DFG) through the Collaborative Research Centre SFB974 (V.K., D.H.). Work on ABCB4 was funded by BMBF through HiChol (01GM1904A, V.K.). K.S. reports funding through Swiss National Science Foundation (SNSF 31003A_125487). S.N. acknowledge funding by the Sonderforschungsbereich SFB/TR 209 "Liver cancer" of the DFG. S.N. acknowledges funding from the DFG im Rahmen der Exzellenzstrategie des Bundes und der Laender EXC 2180 – 390900677 and EXC 2124 – 390838134. MT received funding through the Austrian Science Foundation (FWF) projects F7310 and I2755. M.H. was supported by an ERC Consolidator grant (HepatoMetaboPath), SFBTR179 Project-ID 272983813, SFB/TR 209 Project-ID 314905040, SFBTR1335 Project-ID 360372040, the Wilhelm Sander-Stiftung, the Rainer Hoenig Stiftung, a Horizon 2020 grant (Hepcar), Research Foundation Flanders (FWO) under grant 30826052 (EOS Convention MODEL-IDI).

Conflict of interest
MR, LS, CK, KF, JS, KD, JH, EL, JV, SFG, GH, SJF, IE, DN, CDF, MGB, GG, SV, JPM, MV, KS, TL, KK, DH, TL, MH have nothing to disclose.VK has served as speaker for Falk Foundation, Albireo and Abbvie. JRH has served on the advisory board for Novartis and Orkla Health. JRH has received research support from Biogen unrelated to the current work. THK has received consulting/speaker reimbursement from Gilead and Intercept unrelated to the current work. CS has served as speaker for Falk Foundation. MT has served as speaker for Falk Foundation, Gilead, Intercept and MSD; he has advised for Albireo, BiomX, Boehringer Ingelheim, Falk Pharma GmbH, Genfit, Gilead, Intercept, Jannsen, MSD, Novartis, Phenex, Regulus and Shire. MT further received travel grants from Abbvie, Falk, Gilead and Intercept and research grants from Albireo, Cymabay, Falk, Gilead, Intercept, MSD and Takeda. MT is also co-inventor of patents on the medical use of NorUDCA filed by the Medical Universities of Graz and Vienna (WO2006119803, WO20099013334). PF received norUDCA, an unrestricted research grant, travel grants and advisory board fees from Dr. Falk Pharma GmbH. PF is listed as co-inventor of patents for the medical use of norUDCA filed by the Medical University of Graz (WO2006119803, WO20099013334). UB received grants for investigator-initiated studies by Dr Falk GmbH, Freiburg, and Intercept, San Diego.

Authors' contributions
Conceptualization and design of study (VK, MR, LS, JS, GH, SJF, PF). Data generation (MR, LS, CK, JH, KD, JS, IE, EL, GH, CS, KF, GG, TL, CDF, JPM, MV, MGB, JV), single cell data analysis (GG, SN, TL, KK, JPM), data analysis and interpretation (VK, MR, LS, JS, CW, CK, IE, THK, JRH, DH, TL, SN, MH, MGB, KK, MT). Manuscript preparation (VK, MR, KF, CK, IE, MH, SN, GG, MGB), Critical review and editing (VK, CS, IE, DH, GH, THK, UB, JRH, SJF, DN, PF, GG, KS, TL, MH, MGB, KK, MT), Funding (VK, DH, MH, SN, MT).

Data availability statement
The single-cell RNA sequencing data for this project was deposited on GEO under accession number GSE168758, and SRA under accession number PRJNA713826. Data generated/analyzed during this study are included in the article and its supplementary information and can also be obtained from the corresponding author on reasonable request.

Acknowledgements
Expert technical assistance by Paulina Philippski and Stefanie Lindner is gratefully acknowledged. We thank Sören Weidemann, Institute for Pathology, UKE Hamburg, for providing liver tissue sections. We would like to acknowledge the support of the Biobank of the University Hospital Duesseldorf, Germany.

Supplementary data
Supplementary data to this article can be found online at https://doi.org/10.1016/j.jhep.2021.03.029.

References
Author names in bold designate shared co-first authorship

[1] Dyson JK, Beuers U, Jones DEJ, Lohse AW, Hudson M. Primary sclerosing cholangitis. Lancet 2018;391:2547–2559.
[2] Karlsen TH, Folseraas T, Thorburn D, Vesterhus M. Primary sclerosing cholangitis - a comprehensive review. J Hepatol 2017;67:1298–1323.
[3] Lazaridis KN, LaRusso NF. Primary sclerosing cholangitis. N Engl J Med 2016;375:1161–1170.
[4] Fickert P, Fuchsbichler A, Wagner M, Zollner G, Kaser A, Tilg H, et al. Regurgitation of bile acids from leaky bile ducts causes sclerosing cholangitis in Mdr2 (Abcb4) knockout mice. Gastroenterology 2004;127:261–274.
[5] O'Hara SP, Karlsen TH, LaRusso NF. Cholangiocytes and the environment in primary sclerosing cholangitis: where is the link? Gut 2017;66:1873–1877.
[6] **Tabibian JH**, **O'Hara SP**, Splinter PL, Trussoni CE, LaRusso NF. Cholangiocyte senescence by way of N-ras activation is a characteristic of primary sclerosing cholangitis. Hepatology 2014;59:2263–2275.
[7] **Fickert P**, **Pollheimer MJ**, Beuers U, Lackner C, Hirschfield G, Housset C, et al. Characterization of animal models for primary sclerosing cholangitis (PSC). J Hepatol 2014;60:1290–1303.
[8] Fickert P, Fuchsbichler A, Marschall HU, Wagner M, Zollner G, Krause R, et al. Lithocholic acid feeding induces segmental bile duct obstruction and destructive cholangitis in mice. Am J Pathol 2006;168:410–422.
[9] Kawamata Y, Fujii R, Hosoya M, Harada M, Yoshida H, Miwa M, et al. A G protein-coupled receptor responsive to bile acids. J Biol Chem 2003;278:9435–9440.
[10] Maruyama T, Miyamoto Y, Nakamura T, Tamai Y, Okada H, Sugiyama E, et al. Identification of membrane-type receptor for bile acids (M-BAR). Biochem biophysical Res Commun 2002;298:714–719.
[11] **Sato H**, **Macchiarulo A**, Thomas C, Gioiello A, Une M, Hofmann AF, et al. Novel potent and selective bile acid derivatives as TGR5 agonists: biological screening, structure-activity relationships, and molecular modeling studies. J Med Chem 2008;51:1831–1841.
[12] Perino A, Demagny H, Velazquez-Villegas LA, Schoonjans K. Molecular physiology of bile acid signaling in Health, disease and aging. Physiol Rev 2020.
[13] Deutschmann K, Reich M, Klindt C, Dröge C, Spomer L, Häussinger D, et al. Bile acid receptors in the biliary tree: TGR5 in physiology and disease. Biochim Biophys Acta 2018;1864:1319–1325.
[14] Keitel V, Cupisti K, Ullmer C, Knoefel WT, Kubitz R, Häussinger D. The membrane-bound bile acid receptor TGR5 is localized in the epithelium of human gallbladders. Hepatology 2009;50:861–870.
[15] Keitel V, Ullmer C, Häussinger D. The membrane-bound bile acid receptor TGR5 (Gpbar-1) is localized in the primary cilium of cholangiocytes. Biol Chem 2010;391:785–789.
[16] Masyuk AI, Huang BQ, Radtke BN, Gajdos GB, Splinter PL, Masyuk TV, et al. Ciliary subcellular localization of TGR5 determines the cholangiocyte

functional response to bile acid signaling. Am J Physiol Gastrointest Liver Physiol 2013;304:G1013–G1024.
[17] Reich M, Deutschmann K, Sommerfeld A, Klindt C, Kluge S, Kubitz R, et al. TGR5 is essential for bile acid-dependent cholangiocyte proliferation in vivo and in vitro. Gut 2016;65:487–501.
[18] Beuers U, Hohenester S, de Buy Wenniger LJ, Kremer AE, Jansen PL, Elferink RP. The biliary HCO(3)(-) umbrella: a unifying hypothesis on pathogenetic and therapeutic aspects of fibrosing cholangiopathies. Hepatology 2010;52:1489–1496.
[19] **Hohenester S**, **Wenniger LM**, Paulusma CC, van Vliet SJ, Jefferson DM, Elferink RP, et al. A biliary HCO3- umbrella constitutes a protective mechanism against bile acid-induced injury in human cholangiocytes. Hepatology 2012;55:173–183.
[20] Keitel V, Reich M, Häussinger D. TGR5: pathogenetic role and/or therapeutic target in fibrosing cholangitis? Clin Rev Allergy Immunol 2015;48:218–225.
[21] Li T, Holmstrom SR, Kir S, Umetani M, Schmidt DR, Kliewer SA, et al. The G protein-coupled bile acid receptor, TGR5, stimulates gallbladder filling. Mol Endocrinol 2011;25:1066–1071.
[22] Merlen G, **Kahale N**, **Ursic-Bedoya J**, Bidault-Jourdainne V, Simerabet H, Doignon I, et al. TGR5-dependent hepatoprotection through the regulation of biliary epithelium barrier function. Gut 2020;69:146–157.
[23] Franke A, Balschun T, Karlsen TH, Sventoraityte J, Nikolaus S, Mayr G, et al. Sequence variants in IL10, ARPC2 and multiple other loci contribute to ulcerative colitis susceptibility. NatGenet 2008;40:1319–1323.
[24] Karlsen TH, Franke A, Melum E, Kaser A, Hov JR, Balschun T, et al. Genome-wide association analysis in primary sclerosing cholangitis. Gastroenterology 2010;138:1102–1111.
[25] Thomas C, Gioiello A, Noriega L, Strehle A, Oury J, Rizzo G, et al. TGR5-mediated bile acid sensing controls glucose homeostasis. Cell Metab 2009;10:167–177.
[26] Liaskou E, Jeffery LE, Trivedi PJ, Reynolds GM, Suresh S, Bruns T, et al. Loss of CD28 expression by liver-infiltrating T cells contributes to pathogenesis of primary sclerosing cholangitis. Gastroenterology 2014;147. 221-232 e227.
[27] Soroka CJ, Assis DN, Alrabadi LS, Roberts S, Cusack L, Jaffe AB, et al. Bile-derived organoids from patients with primary sclerosing cholangitis recapitulate their inflammatory immune profile. Hepatology 2019;70:871–882.
[28] Dorrell C, Erker L, Schug J, Kopp JL, Canaday PS, Fox AJ, et al. Prospective isolation of a bipotential clonogenic liver progenitor cell in adult mice. Genes Dev 2011;25:1193–1203.
[29] Schaub JR, Huppert KA, Kurial SNT, Hsu BY, Cast AE, Donnelly B, et al. De novo formation of the biliary system by TGFbeta-mediated hepatocyte transdifferentiation. Nature 2018;557:247–251.
[30] Team RC. R: a language and environment for statistical computing. R Foundation for Statistical Computing; 2017 [cited 2017; Available from: https://www.R-project.org/.
[31] Satija R, Farrell JA, Gennert D, Schier AF, Regev A. Spatial reconstruction of single-cell gene expression data. Nat Biotechnol 2015;33:495–502.
[32] McInnes L, Healy J, Melville J. UMAP: uniform manifold approximation and projection for dimension reduction. 2018. ArXiv e-prints 180203426.
[33] Chen YY, Arndtz K, Webb G, Corrigan M, Akiror S, Liaskou E, et al. Intrahepatic macrophage populations in the pathophysiology of primary sclerosing cholangitis. JHEP Rep 2019;1:369–376.
[34] **Guicciardi ME**, **Trussoni CE**, Krishnan A, Bronk SF, Lorenzo Pisarello MJ, O'Hara SP, et al. Macrophages contribute to the pathogenesis of sclerosing cholangitis in mice. J Hepatol 2018;69:676–686.
[35] **Tabibian JH**, **Trussoni CE**, O'Hara SP, Splinter PL, Heimbach JK, LaRusso NF. Characterization of cultured cholangiocytes isolated from livers of patients with primary sclerosing cholangitis. Lab Invest 2014;94:1126–1133.
[36] Ferreira-Gonzalez S, Lu WY, Raven A, Dwyer B, Man TY, O'Duibhir E, et al. Paracrine cellular senescence exacerbates biliary injury and impairs regeneration. Nat Commun 2018;9:1020.
[37] Vesterhus M, Holm A, Hov JR, Nygard S, Schrumpf E, Melum E, et al. Novel serum and bile protein markers predict primary sclerosing cholangitis disease severity and prognosis. J Hepatol 2017;66:1214–1222.
[38] Zweers SJ, Shiryaev A, Komuta M, Vesterhus M, Hov JR, Perugorria MJ, et al. Elevated interleukin-8 in bile of patients with primary sclerosing cholangitis. Liver Int 2016;36:1370–1377.
[39] Klindt C, Reich M, Hellwig B, Stindt J, Rahnenfuhrer J, Hengstler JG, et al. The G protein-coupled bile acid receptor TGR5 (Gpbar1) modulates endothelin-1 signaling in liver. Cells 2019;8.
[40] MacParland SA, Liu JC, Ma XZ, Innes BT, Bartczak AM, Gage BK, et al. Single cell RNA sequencing of human liver reveals distinct intrahepatic macrophage populations. Nat Commun 2018;9:4383.
[41] Aizarani N, Saviano A, Sagar, Mailly L, Durand S, Herman JS, et al. A human liver cell atlas reveals heterogeneity and epithelial progenitors. Nature 2019;572:199–204.
[42] Pepe-Mooney BJ, Dill MT, Alemany A, Ordovas-Montanes J, Matsushita Y, Rao A, et al. Single-cell analysis of the liver epithelium reveals dynamic heterogeneity and an essential role for YAP in homeostasis and regeneration. Cell Stem Cell 2019;25:23–38 e28.
[43] Ramachandran P, Dobie R, Wilson-Kanamori JR, Dora EF, Henderson BEP, Luu NT, et al. Resolving the fibrotic niche of human liver cirrhosis at single-cell level. Nature 2019;575:512–518.
[44] Lazaridis KN, Strazzabosco M, Larusso NF. The cholangiopathies: disorders of biliary epithelia. Gastroenterology 2004;127:1565–1577.
[45] Fickert P, Wagner M, Marschall HU, Fuchsbichler A, Zollner G, Tsybrovskyy O, et al. 24-norUrsodeoxycholic acid is superior to ursodeoxycholic acid in the treatment of sclerosing cholangitis in Mdr2 (Abcb4) knockout mice. Gastroenterology 2006;130:465–481.
[46] Fickert P, Hirschfield GM, Denk G, Marschall H-U, Altorjay I, Färkkilä M, et al. norUrsodeoxycholic acid improves cholestasis in primary sclerosing cholangitis. J Hepatol 2017;67:549–558.
[47] **Tabibian JH**, **O'Hara SP**, Trussoni CE, Tietz PS, Splinter PL, Mounajjed T, et al. Absence of the intestinal microbiota exacerbates hepatobiliary disease in a murine model of primary sclerosing cholangitis. Hepatology 2016;63:185–196.
[48] Bessho K, Mourya R, Shivakumar P, Walters S, Magee JC, Rao M, et al. Gene expression signature for biliary atresia and a role for interleukin-8 in pathogenesis of experimental disease. Hepatology 2014;60:211–223.
[49] Dong R, Zheng S. Interleukin-8: a critical chemokine in biliary atresia. J Gastroenterol Hepatol 2015;30:970–976.
[50] Baghdasaryan A, Claudel T, Gumhold J, Silbert D, Adorini L, Roda A, et al. Dual farnesoid X receptor/TGR5 agonist INT-767 reduces liver injury in the Mdr2-/- (*Abcb4*-/-) mouse cholangiopathy model by promoting biliary HCO(-)(3) output. Hepatology 2011;54:1303–1312.
[51] Halilbasic E, Fiorotto R, Fickert P, Marschall H-U, Moustafa T, Spirli C, et al. Side chain structure determines unique physiologic and therapeutic properties of norursodeoxycholic acid in Mdr2−/− mice. Hepatology 2009;49:1972–1981.
[52] Sombetzki M, Fuchs CD, Fickert P, Osterreicher CH, Mueller M, Claudel T, et al. 24-nor-ursodeoxycholic acid ameliorates inflammatory response and liver fibrosis in a murine model of hepatic schistosomiasis. J Hepatol 2015;62:871–878.